American Journal of Aerospace Engineering
2018; 5(1): 1-8
http://www.sciencepublishinggroup.com/j/ajae
doi: 10.11648/j.ajae.20180501.11
ISSN: 2376-4813 (Print); ISSN: 2376-4821 (Online)

Optical Parameters and Electrical Transport Properties of Some Barium-Sodium-Borate Glasses Doped Bismuth Oxide

Sayed M. Salem[1], Taha Z. Abou-Elnasr[1], Wael A. El-Gammal[2], Ahmed S. Mahmoud[1], Heba A. Saudi[1, *], Ahmed G. Mostafa[1]

[1]Physics Department, Faculty of Science, Al-Azhar University, Cairo, Egypt

[2]Egyptian Nuclear & Radiological Regulatory Authority, Cairo, Egypt

Email address:

heba_saudi@hotmail.com (H. A. Saudi)

[*]Corresponding author

To cite this article:

Sayed M. Salem, Taha Z. Abou-Elnasr, Wael A. El-Gammal, Ahmed S. Mahmoud, Heba A. Saudi, Ahmed G. Mostafa. Optical Parameters and Electrical Transport Properties of Some Barium-Sodium-Borate Glasses Doped Bismuth Oxide. *American Journal of Aerospace Engineering*. Vol. 5, No. 1, 2018, pp. 1-8. doi: 10.11648/j.ajae.20180501.11

Received: January 4, 2018; **Accepted**: January 22, 2018; **Published**: February 7, 2018

Abstract: Glasses having the composition, [(70-x) mol% B_2O_3- x mol% Bi_2O_3- 10 mol% BaO- 20 mol% Na_2O, where 0≤ x ≤20], have been prepared by the melt quenching method. Density, molar volume, infrared analysis, optical parameters and Electrical properties have been thoroughly investigated. It was found that, both density and molar volume increased with the gradual replacement of B_2O_3 by Bi_2O_3 and the comparison between their experimental and empirical values confirm the amorphous nature and the random structure of all samples. The obtained infrared results indicated that different structural borate groups appeared such as BO_4 units (in di-, tri- and penta-borate groups) and BO_3 units (in meta- and ortho-borate chains). Also, both BiO_3 and BiO_6 are present in all Bi doped glasses, and the BiO_3 / BiO_6 ratio appeared to be approximately stable as Bi_2O_3 was increased to 15 mol%, then it showed a jump increase when BiO_3 reached 20 mol%. The optical band gap energy and cut-off wavelength increased with the increase of Bi_2O_3 while Urbach energy decreased. On the other hand, the electrical conductivity decreased as Bi_2O_3 was gradually replaced by B_2O_3, while the activation energy increased and all samples exhibit semi-conductors behavior and the values of the exponent factor decreased gradually with temperature, which is compatible with the correlated barrier hopping conduction mechanism.

Keywords: Sodium-Borate Glasses, FTIR, Optical Parameters, AC Conductivity

1. Introduction

The study of heavy metal doped various glasses appeared now of high interest. These glasses exhibit different important physical and chemical properties (such as: high refractive index, high IR transparency, high density, good shielding parameters for ionizing radiation…etc.) [1]. However, they mostly found interesting technological applications in various daily life fields (such as: layers for opto-electronic devices, reflecting windows, thermal- and mechanical-sensors …etc.) [2].

On the other hand, borate glasses are considered now as one of the most important solid materials and boron are classified as interesting glass former cation. The structure of such glasses as well as their structural transformations due to the variation of their chemical composition and additives, are -far away- thoroughly investigated, and they become -nowadays- well known [1, 3-5]. However, it is well known that, boron atoms in borate glasses are usually coordinated either to three or four oxygen atoms forming [BO_3] or [BO_4] structural units, depending on the concentration of the added modifier cations. These two fundamental units can be combined to form some super-structure unites (like boroxol ring, pentaborate,

tetraborate, diborate groups … etc.) [2, 6-8].

The properties of borate glasses modified with alkali oxide show a nonlinear behavior when alkali oxide was gradually increased. This departure from linearity is termed as boron anomaly phenomenon. There are numerous studies on such boron anomaly phenomenon utilizing electrical conductivity during glass network, infrared spectroscopy and neutron diffraction techniques ….ect. [9].

However, in this article, some barium-sodium-borate glasses doped different amounts of bismuth oxide (at the expense boron oxide) have been prepared. The effect of the gradual replacing of B_2O_3 by Bi_2O_3 on the density, molar volume, electrical transport properties and optical parameters, of the prepared solid glasses has been thoroughly studied. In addition, the obtained glasses were subjected also to FTIR spectral analysis, in order to get information about the internal structural groups in the glass networks.

2. Experimental Work

A glass system having the composition [(70-x) mol% B_2O_3 - x mol% Bi_2O_3 -10 mol% BaO - 20 mol% Na_2O, where $0 \leq x \leq 20$] has been prepared by the melt quenching method. The raw materials were mixed well in an agate mortar, and were then transferred into porcelain crucibles. The batches were melted in an electric muffle furnace exacted at 1200 ºC for two hours. Melts were stirred several times during melting to ensure complete mixing and homogeneity. After the duration of melting they were poured on a stainless steel plate at room temperature. The obtained samples are examined visually where, they all appeared transparent and exhibit pure glassy state.

Archimedes technique was used to measure the experimental density by weighting a solid sample in air and in an immersion liquid (of stable density) at room temperature and the experimental density values was calculated according to Archimedes equation. Then the empirical density values were also calculated form the corresponding close packed structure of the same composition and the variations of both density values are exhibited in the same figure for comparison [10].

Molar volume values are usually considered to be more sensitive to reflect the structural variations between the prepared glass samples as well as between glasses and their corresponding crystalline materials than density. They also normalize the atomic weights of different glass constituents [11]. Therefore, the molar volume values (experimentally and empirically) were also calculated [6].

Infrared (IR) spectroscopic analysis was used to obtain information about the internal structur groups forming a glass network. The IR spectra of the studied glasses are obtained at RT in the range from 4000 to 400 cm^{-1} by using Fourier Transform Infra-red spectrometer (type Perken Elmer, model RTX). KBr disk technique was used, where 2 mg of the sample under test was weighted and mixed well with about 200 mg KBr and was then pressed to form disk shape sample suitable for IR measurements.

The optical parameters were then obtained by measuring their transmission (T) spectra using a Carel Zeiss-PMQ spectrometer. The measurements were carried out at room temperature in the spectral range from 190 to 1100 nm. The used source was a deuterium lamp used in the range 285-325 nm (at shorter wavelength) and a tungsten lamp used in the range 325-2500 nm (in the visible and near infrared regions).

For electrical measurements, the solid glasses were polished to obtain disk shape samples with 7 mm diameter and 1 mm thickness. The ac conductivity measurements were performed using LRC bridge (model SR 270) at four fixed frequencies (0.120, 1, 10, 100 kHz). The samples must be cleaned and sandwiched between two electrodes of silver paste to obtain good electrical contact.

3. Results and Discussion

3.1. Density (ρ) and Molar Volume (V_m)

Although the visual examination of the prepared samples showed that all samples are transparent and hence reflecting the amorphous nature and randomness character, density (ρ) and molar volume (V_m) values (experimentally and empirically) were obtained in order to confirm the amorphous nature for all samples. All the obtained results are listed in Table 1.

From this table, it can be seen that both the empirical and the experimental density values increased gradually with the gradual increase of Bi_2O_3. It is observed also that, the empirical density values are absolutely higher than those obtained experimentally. This can be attributed to the high density value of Bi_2O_3 (8.9 g/cm^3) which is much greater than that of B_2O_3 (2.56 g/cm^3). Therefore, the density has to increase gradually and logically when Bi_2O_3 was gradually introduced replacing B_2O_3.

It is seen also that, both molar volume (V_m) values increased gradually with the gradual increase of Bi_2O_3 content, and the empirical values exhibit lowed values than those obtained experimentally. Such increase of Vm may be due to the ionic radius of Bi^{3+} (1.6 Å) which is greater than the ionic radius of B^{3+} (0.85 Å). That is, the ionic radius of Bi^{3+} is approximately twice that of $B^{3+.}$ However, it can be concluded that, the gradual replacing of boron by the bismuth act to increase gradually the molar volume of the studied glasses.

The higher empirical density values than the corresponding experimental ones and the higher experimental molar volume values than those of the corresponding empirical ones can be taken as evidences for the amorphous nature and the random character of all the studied samples [12].

Table 1. *The experimental and empirical values of both density and molar volume as well as Bio_3/Bio_6 ratio.*

Bi_2O_3 mol %	ρ_{exp} (gm/cm^3)	ρ_{emp} (gm/cm^3)	$V_{m\ exp}$ (cm^3/mol)	V_{memp} (cm^3/mol)	BiO_3/BiO_6
0	2.19	2.81	34.89	27.13	0
5	2.40	3.13	40.08	30.71	1.30
10	2.77	3.45	41.76	33.63	1.32
15	3.05	3.76	44.51	36.06	1.28
20	3.39	4.08	45.81	38.11	1.46

3.2. FTIR Spectroscopy

It is of interest to obtain information about the internal structure of the studied glasses. However, infrared spectroscopic analysis was applied here to inspect the internal structure of the studied glass networks. Therefore, figure 1 shows the obtained IR spectra of all glasses in the range from 400 to 4000 cm^{-1}.

It is appeared that, the range of interest is only between 400 and 2000 cm^{-1}, since all bands appeared in the range from 2000 to 4000 cm^{-1} are attributed to OH, H-O-H and hydrogen-bond vibrations. Also the band appeared in between 1600 and 1770 cm^{-1} in all glasses can be attributed to the stretching vibration of H-O bond [13]. The appearance of these bands evidenced the presence of some moisture absorbed from the environmental air, which may be due the used KBr disk technique [14-16]. Accordingly, the range from 400 to 2000 cm^{-1} was thoroughly examined by applying the de-convolution program to extract, as real as possible, the correct IR bands. Therefore,

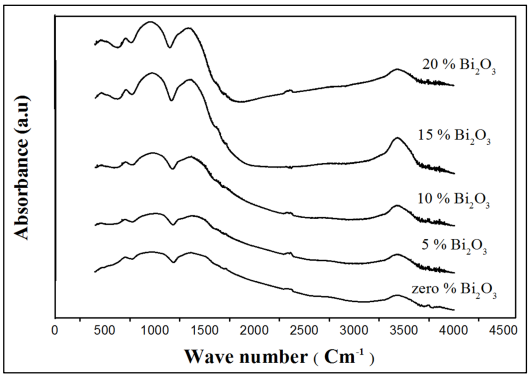

Figure 1. *The as measured IR spectra of all samples.*

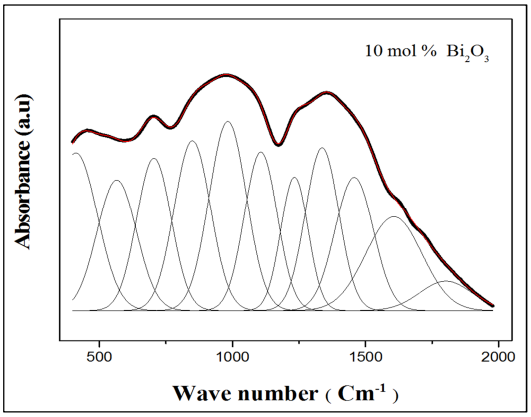

Figure 2. *The de-convoluted spectrum of the sample contains 10 mol% Bi_2O_3, as a representative spectrum.*

It was found that some major IR bands appeared in the de-convoluted spectra of all the studied glasses where these bands can be attributed to the vibrations of some structural groups or chemical bonds in the glass networks. The vibrations of these bands and their attributance can be summarized as follows:

1. The band appeared around 426 cm^{-1} may be due to, two overlapped bands, the first one is due to the bending vibration of Bi-O bonds in BiO_3 polyhedra [17], while the second one may be due to the specific vibrations of Ba-O bonds [18, 19]. For the Bi free sample, this band is only due to the specific vibrations of Ba-O bonds.
2. The band appeared between 562 and 642 cm^{-1} may be due also to two overlapped bands, the first one indicated the presence of the vibration of the Bi–O bond in the BiO_6 (octahedral units) [20], while the second one may be due also to the vibrations of Ba-O bonds [18, 19]. Also, in the Bi_2O_3 free sample, this band is due only to the specific vibrations of Ba-O bonds. From the above mentioned vibrations, it can be concluded that bismuth cations occupy both the glass network former (GNF) and glass network modifier (GNM) position.
3. The band centered approximately at 700 cm^{-1} may be due to the bending vibration of B-O-B in BO_3 triangles and the intensity of this band seems to decrease with the gradual increase of Bi_2O_3 content [20, 21].
4. The bands appeared in the region from 775 to 1190 cm^{-1} can be attributed to the stretching vibration of B–O bonds in the tetrahedral boron units (BO_4) occurred in tri-borate, di-borate and penta-borate groups [21].
5. The band appeared between 824 and 855 cm^{-1} (except the first sample) can be attributed to the presence of BiO_3 polyhedral units [22-23].
6. The group of bands, which occur in the ringe from 1210 to 1540 cm^{-1} is due to the asymmetric stretching vibration of the B–O bonds in BO_3 units, and the peak that appeared between 1208 cm^{-1} and 1240 cm^{-1} is due to B–O stretching vibration in BO_3 units in meta- and ortho-borate chains. The peak appeared between 1291 and 1336 cm^{-1} is due to the asymmetric stretching vibration of B–O bond in BO_3 trigonal units [24].
7. The band appeared between 1433 and 1491 cm^{-1} may be related to B–O stretching vibration $(BO_3)^{3-}$ units in meta- and ortho-borates chains [25].

However, the IR results indicated that, many structural groups due to boron ions appeared such as BO_4 units in tri-, di- and penta-borate groups as well as BO_3 units in meta- and ortho-borate chains. All the present sodium and barium cations participate as glass network modifier (GNM). According to the

area under the observed bands due to BiO_3 and BiO_6, it is seen that, as Bi_2O_3 was increased the ratio of BiO_3/BiO_6 appeared to be stable up to Bi_2O_3=15 mol%. But exceeding such value of Bi_2O_3 and reaching 20 mol%, such ratio shows a jump increase (see Table 1). This means that Bi cations transfer gradually from GNM to glass network former (GNF) positions.

3.3. Optical Properties

The optical transitions and electronic band structure of the studied glasses were thoroughly investigated in the UV- VIS region, and Figure 3, shows the optical transmission spectra, as a function of the wavelength in the range from 190 to 1100 nm at room temperature. From this figure, the optical absorption edge ($\lambda_{cut\text{-}off}$) can be obtained from the intersection point of each spectrum (of a certain sample) with λ axis.

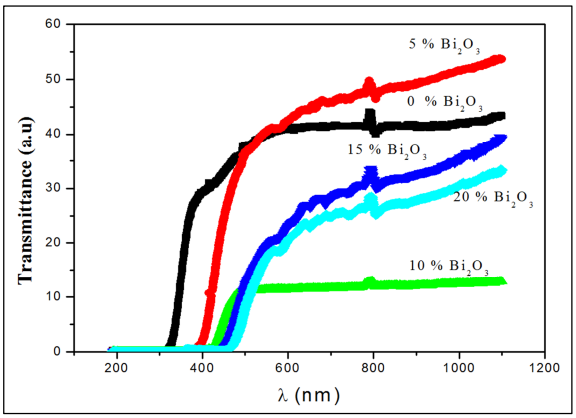

Figure 3. *The optical transmission spectra for all samples as a function of wavelength.*

The variation of $\lambda_{cut\text{-}off}$ values as a function of Bi_2O_3 content can be shown in Figure 4. Omitting the value due to the Bi_2O_3 free sample, it appeared that the cut-off wavelength exhibits gradual linear increase. Since the absorption edge is generally determined by the strength of oxygen bond in the glass networks, therefore it can be stated that, the gradual increase of Bi_2O_3 act to strengthening the glass networks, that is the introduced Bi^{3+} cation act to produce a glass network of higher strength [26].

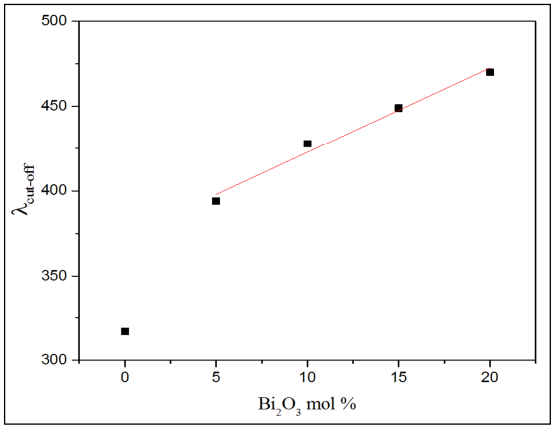

Figure 4. *The variation of the cut-off wavelength ($\lambda_{cut\text{-}off}$) versus Bi_2O_3 content.*

The absorption coefficient, α (hν), near the edge of each spectrum was calculated using the following equation

$$\alpha(h\upsilon) = \frac{1}{d}\ln\left(\frac{I_o}{I_t}\right) \quad (1)$$

Where d is the thickness of the sample under investigation, I_o and I_t are the intensities of the incident and transmitted radiations respectively.

Mott and Davis had proposed equation (2) for amorphous materials [27],

$$\alpha\, h\upsilon = B\,(h\upsilon - E_{opt})^r \quad (2)$$

Where E_{opt} is the optical band gap, B is a constant called the band tailing parameter, hυ is the incident photon energy and r is an index, takes the values (2, 3, 1/2 or 3/2) corresponding to indirect allowed, indirect forbidden, direct allowed and direct forbidden transitions respectively. Equation (2) must depicts a straight line, and r must be equal 2, since the indirect allowed transition is the most probable transition in all amorphous solid.

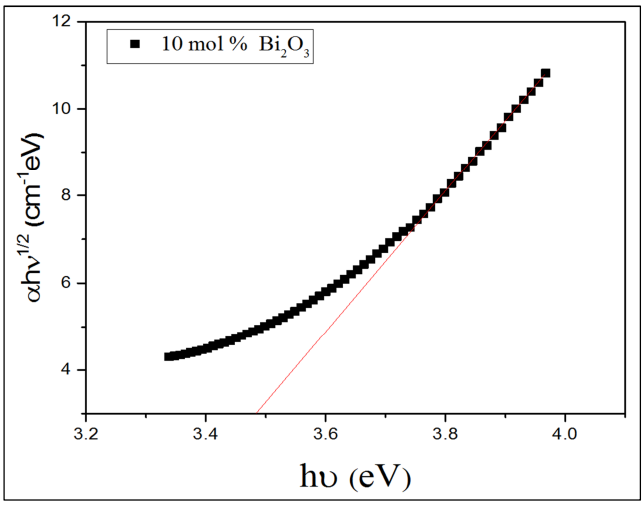

Figure 5. *$(\alpha h\upsilon)^{1/2}$ as a function of photon energy (hυ) (Tauc plot) for the sample containing 10 mol% Bi_2O_3, as a representative figure.*

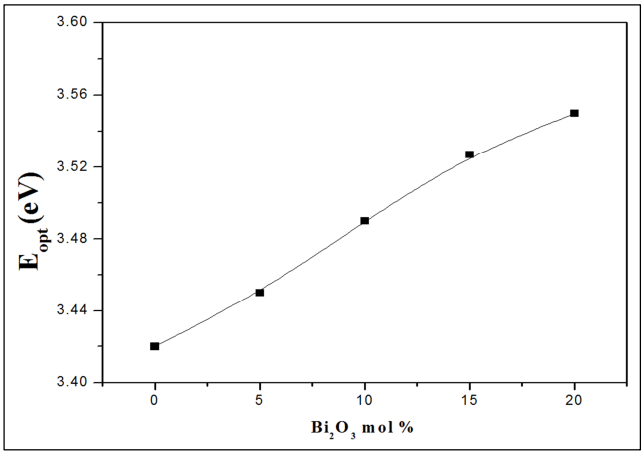

Figure 6. *The variation of the optical band gap energy (E_{opt}) versus Bi_2O_3 content.*

Figure 5 represents the variation of $(\alpha h\upsilon)^{1/2}$ with the photon hυ (Tauc plot), for the sample containing 10 mol% Bi_2O_3, as a representative figure. The values of E_{opt} for all samples have been calculated by extrapolating the linear portion of the curves to intersect at $(\alpha h\upsilon)^{1/2} = 0$.

On the other hand, Figure 6 exhibits the variation of the optical band gap energy (E_{opt}) for the allowed indirect transition as a function of Bi_2O_3. It appeared that, E_{opt} values increased gradually and linearly with the increase of Bi_2O_3 content, which is probably related to the increase in the average number of bridging oxygen atoms in the glass network [28].

To calculate the width of the energy band tail (Urbach energy (ΔE_U)) of the density of states, the model proposed by Urbach can be followed [26] applying the following equation,

$$\alpha (h\upsilon) = \alpha_o \exp (h\upsilon/\Delta E_U) \quad (3)$$

Where α_o is a constant, ΔE_U is Urbach energy which indicates the width of the band tails of the localized states representing the degree of disorder in amorphous and crystalline systems. Consequently, the defect concentration can be also obtained by measuring Urbach energy [26]. Therefore, Figure 7 shows the variation of (ln α) against (hυ) for the sample containing 10 mol % Bi_2O_3 as a representative figure. The values of Urbach energy (ΔE_U) have been calculated from the reciprocal of the slope of the linear portion of these curves.

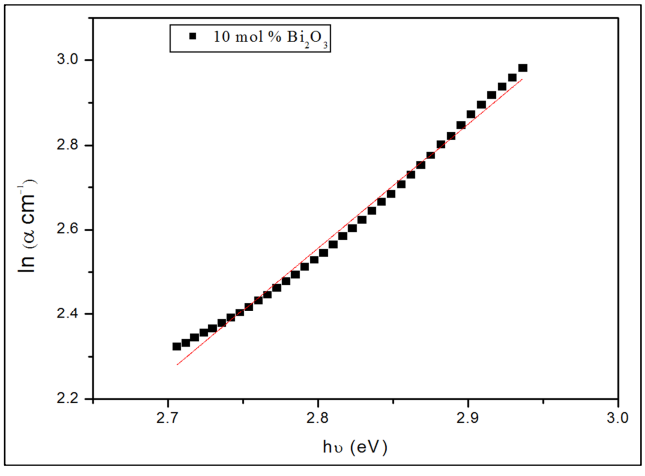

Figure 7. *ln α as a function of the photon energy (hυ) for the sample containing 10 mol% Bi_2O_3, as a representative figure.*

From another point of view, Figure 8 shows the change in the Urbach energy (ΔE_U) as a function of Bi_2O_3 content. The origin of Urbach energy in amorphous materials may be the stronger broadening of absorption edge compared with crystals. This origin can be attributed to the lack of long range order. It was found that Urbach energy decreases linearly with increasing Bi_2O_3 which reveals the decrease of the degree of disorder with the gradual substitution of B_2O_3 by Bi_2O_3 cations. Moreover, the increase in E_{opt} and the decrease in Urbach energy with Bi_2O_3 can be attributed to the gradual decrease of the disorder in the studied samples [29, 32].

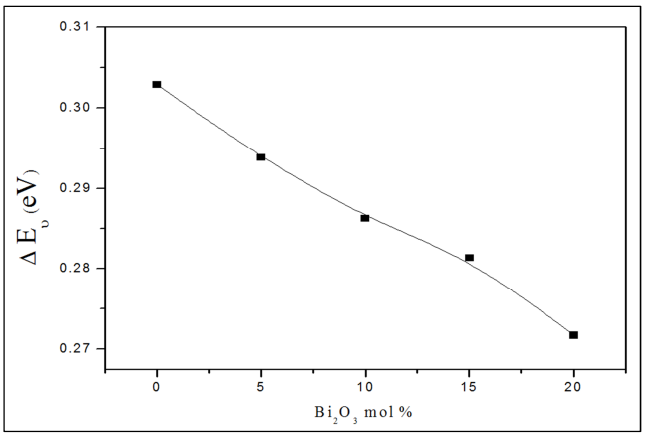

Figure 8. *The variation of Urbach energy (ΔE_υ) versus Bi_2O_3 content.*

However, it can be stated that, as Bi_2O_3 content has gradually increased at the expense of B_2O_3, the optical band gap energy and the cutoff wavelength ($\lambda_{cut\text{-}off}$) increased linearly (when omitting the value due to the bismuth free sample) while Urbach energy decreased which means that the glass network has more strength and the ratio of the disorder character decrease. The obtained values of the studied optical parameters confirm the amorphous nature of the studied samples.

3.4. Electrical Transport Properties

In an ac experiment the measured conductivity represents the sum of the ac and dc conductivities according to equation (4), [33, 34],

$$\sigma_{total} = \sigma (\omega) + \sigma_{dc} \quad (4)$$

The ac conductivity of the disordered solids depends on both frequency and temperature. Elliot had stated that the frequency dependent ac conductivity can be described by the following universal power law (equation 5) [33],

$$\sigma (\omega) = A\, \omega^s \quad (5)$$

where σ (ω) is the ac conductivity, A is a weekly temperature dependent parameter, ω is the angular frequency and s is the exponent factor (usually $s \leq 1$) and is given by,

$$s = \frac{d \ln\sigma(\omega)}{d \ln(\omega)} \quad (6)$$

However the total conductivity has been measured for all samples, as a function of temperature and frequency. The obtained experimental data for the sample contains 10 mol % Bi_2O_3 can be shown in Figure 9 as a representative figure, and all samples exhibit approximately similar behavior. It appeared from this figure that at higher temperatures the total conductivity shows strong temperature dependence and weak frequency dispersion. While at low temperatures, it shows weak temperature dependence and strong frequency dependence. The reason for this behavior is that, the

conductivity has two parts, ac and dc conductivities, where the ac conductivity is frequency dependent, but weakly temperature dependent, while dc conductivity is temperature dependent and frequency independent [35].

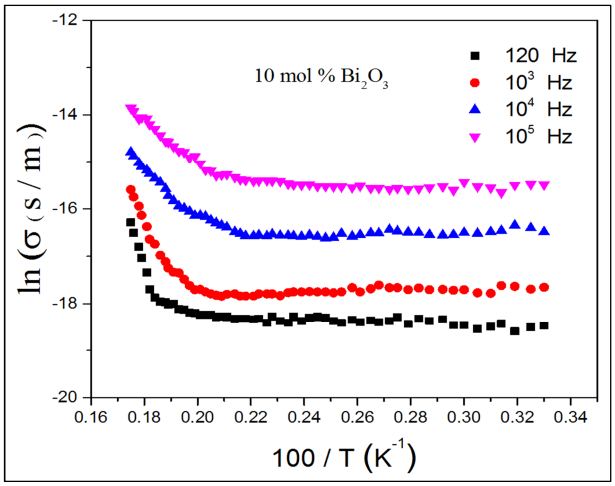

Figure 9. *The total conductivity, temperature dependence at four fixed frequencies for the sample containing 10 mol % Bi_2O_3, as a representative figure.*

Figure 10 shows the variation of $\ln\sigma_t$ as a function of Bi_2O_3 content at different fixed temperatures (353, 433 and 473 K). From such figure, it can be seen that as Bi_2O_3 has gradually increased replacing B_2O_3, the conductivity exhibits gradual decrease. The observed non-linear variation of ln σ versus Bi_2O_3 content may be due to the mixed alkali – alkaline earth effect (Na_2O & BaO). In addition, some of the introduced bismuth cations act either as former or a modifier. Therefore, it can be stated that, there are three different modifier cations (Na^+, Ba^{2+} & Bi^{3+}) as well as two former cations (B^{3+} & Bi^{3+}). All these factors act directly to the non-linear variation of conductivity with Bi_2O_3 content [36].

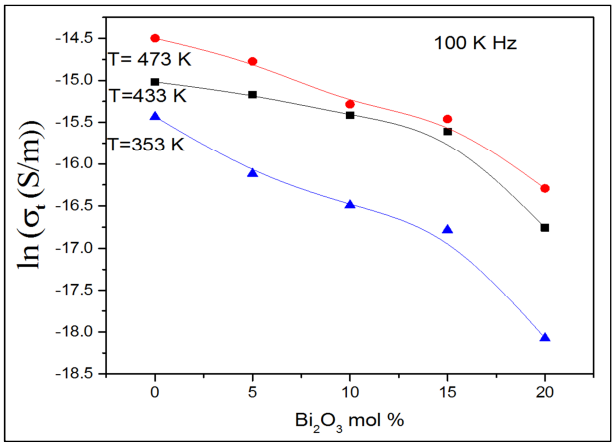

Figure 10. *The total conductivity as a function of Bi_2O_3 content at different fixed temperatures.*

The dc electrical activation energies were calculated by applying Arrhenius equation (no. 7), and figure 11 represents the variation of the obtained values as a function of Bi_2O_3 content.

$$\sigma_{dc} = \sigma_0 \exp(-\Delta E / kT) \quad (7)$$

where σ_0 is the pre-exponential factor and ΔE is the activation energy. The variation of the activation energy with Bi_2O_3 content shows logically the reverse behavior of the conductivity [37].

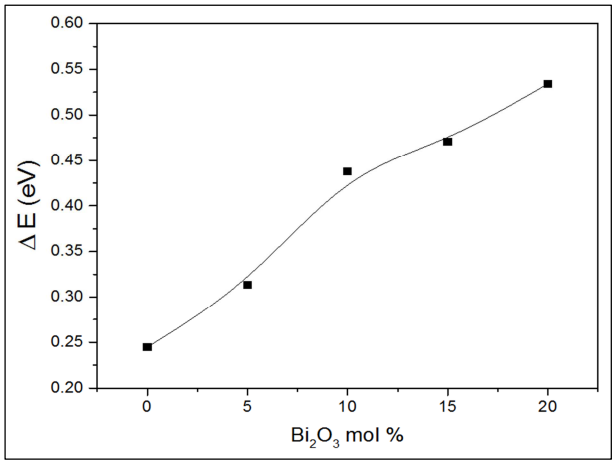

Figure 11. *The variation of the dc electrical activation energy as a function of Bi_2O_3 content.*

The observed decrease of conductivity as well as the gradual increase of the electrical activation energy as B_2O_3 was gradually replaced by Bi_2O_3, may be due to the following factors [37, 38].

a) The blocking effect of the large volume bismuth cation in comparison with the small volume boron cation, since some bismuth cations will act to fill the vacancies leading to block the pathways of the charge carriers and hence leads to an effective decrease in the mobility of the present sodium cations. This was found in agreement with the variation of both molar volume and density of the studies glass samples.

b) Although bismuth cations have two different oxidation states (Bi^{3+} & Bi^{5+}), but the gradual decrease of boron cations may force bismuth cations to occupy the glass former positions, and hence the participation of bismuth cation in the conduction process decreased. This was confirmed by calculating BiO_3/BiO_6 ratio, that obtained from IR analysis.

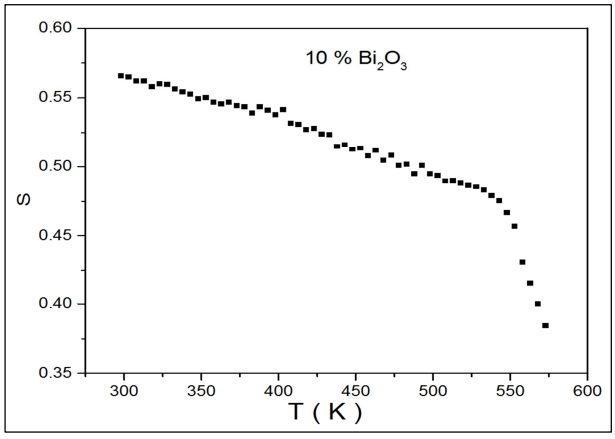

Figure 12. *The variation of S-factor as a function of temperature for the sample containing 10 mol% Bi_2O_3, as a representative figure.*

The values of the exponent factor (S) were then calculated, and figure12, exhibits its variation as a function of temperature, for the sample contain 10 mol% Bi_2O_3 as representative figures. Such variation gives a primary indication about the conduction mechanism through the investigated glasses. It is seen that S-factor decreases with the increase of temperature, which is fitted completely to the correlated barrier hopping (CBH) model, (equation (8)),

$$S = 1 - \frac{6KT}{W_m - KTln(\omega\tau_0)} \quad (8)$$

The dielectric constant (ε') was also investigated for all samples and Figure 13 shows the effect of both frequency and temperature on ε' for the sample containing 10 mol% Bi_2O_3, as a representative figure, and all other samples exhibit approximately similar behavior. From this figure, it is seen that as the temperature was gradually increased, ε' exhibits a stable value (frequency and temperature independent) up to a certain temperature (T_o) differ from one sample to another. Then it starts to increase quickly with temperature such that this increase is inversely proportional to frequency. This behavior can be attributed to the orientational polarization which is directly related to the thermal motion (vibration) of molecules [37] and/or the space charge polarization due to the bonding defects in the structure [38]. The observed variation of ε' with frequency may be due to the fact that as the frequency was increased the orientational polarization decreased since it takes more time than the electronic and ionic polarization [38].

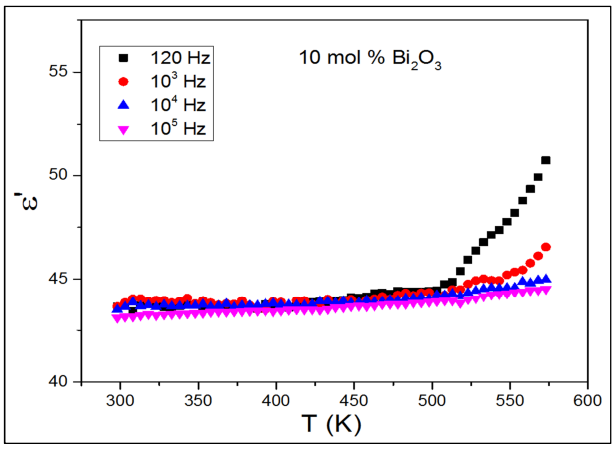

Figure 13. *The dielectric constant temperature dependence of the sample containing 10 mol% Bi_2O_3, as a representative figure.*

On the other hand, figure14 exhibits the variation of the dielectric loss factor (ε'') as a function of temperature at four different frequencies (0.12, 1, 10 and 100 kHz) for the sample containing 10 mol% Bi_2O_3 as a representative figure. All other samples of the studied glasses show approximately similar behavior. It is clear that at low temperature ε'' is frequency and temperature independent, while at high temperature, it increases gradually in such a way that the increment rate is inversely proportional to frequency. This behavior may be due to the relaxation phenomena which can be divided into three parts, the conduction loss, the dipolar loss and the vibrational loss. Since the conduction loss is proportional to σ_t, therefore the loss increased as the conductivity increased [38, 39].

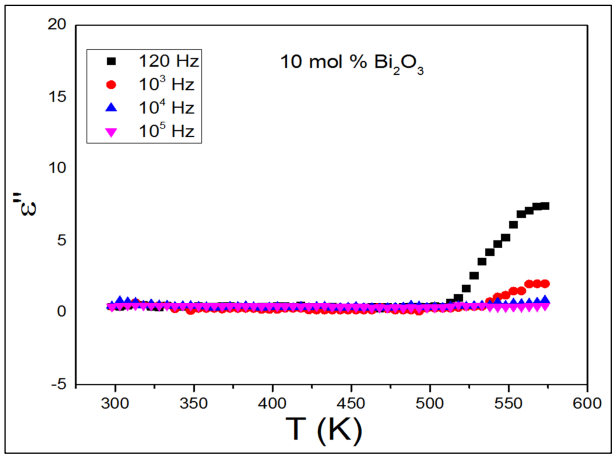

Figure 14. *The dielectric loss factor temperature dependence of the sample containing 10 mol% Bi_2O_3, as a representative figure.*

4. Conclusion

According to the above examinations of the studied glasses, it can be concluded that:

1. Both density and molar volume values increased gradually and linearly with the gradual replacement of B_2O_3 by of Bi_2O_3 content.
2. The comparison between both the experimental and empirical density and molar volume values evidenced the amorphous nature of the studied samples.
3. The IR results evidenced the presence of different structural borate groups. Both BiO_3 and BiO_6 groups are also present through the glass networks except that of the Bi_2O_3 free sample.
4. As B_2O_3 was gradually replaced by Bi_2O_3, the BiO_3/BiO_6 ratio shows approximate stability up to Bi_2O_3=15 mol%, then at 20 mol% it exhibits a jump increase. That is, bismuth cations occupying GNM positions, transferred to occupy the GNF positions.
5. It is concluded that, $\lambda_{cut\text{-}off}$ and E_{opt} increased, with the increase of Bi_2O_3, while Urbach energy decreased.
6. All samples behave like semi-conductors and the total conductivity decreased with the increase of Bi_2O_3, while the electrical activation energy increased.
7. The conduction mechanism of all samples was found in agreement with that of the CBH model.

References

[1] J. E. Shelby, Introduction to Glass Science and Technology, The Royal Society of Chemis try, UK, (1997).

[2] S. Sanghi, S. Duhan, A. Agarwal and P. Aghamkar, J. Alloys and Compounds, 488 (2009) 458.

[3] N. A. Eissa, A. M. Sanad, A. A. El-Saghier, H. A. Sallam and A. G. Mostafa, Acta Physica Hungarica, 59 (1986) 297.

[4] Krough-Moe, J. Phys. Chem. Glasses, 6 (1965) 46.

[5] T. Nishida, M. SuzuKi, S. Kubuki, M. Katata and Y. Maeda, J. Non Cryst. Solids, 194 (1996) 23.

[6] A. Varshneya, "Fundamentals of Inorganic Glasses", Academic Press Inc., New-York, (1994).

[7] T. Yano, N. Kunimine, S. Shibata and M. Yamane, J. Non-Cryst. Solids, 321 (2003) 137.

[8] T. Yano, N. Kunimine, S. Shibata and M. Yamane, J. Non-Cryst. Solids, 321 (2003) 157.

[9] I. Oprea, PhD thesis, Physics Dep., Osnabruck Univ., "Optical Properties of Borate Glass-Ceramics", (2005).

[10] Kulwinder Kaur, K. J. Singh and Vikas Anand, J. Radiation Physics and Chemistry, 120 (2016) 72.

[11] H. El Mkami, J. Phys. Chem. Solids, 61 (2000) 153.

[12] G. S. M. Ahmed, A. S. Mahmoud, S. M. Salem and T. Z. Abo-Elnasr, American J. Phys. & Applications, 3, 4 (2015) 112.

[13] H. A. Saudi, A. Abd-Elalim, T. Z. Abo-Elnasr and A. G. Mostafa, Nature & Science, 13 (2015) 71.

[14] S. A. MacDonald, C. R. Schardt, D. J. Masiello and J. H. Simmons, J. Non-Cryst. Solids, 275 (2000) 72.

[15] A. A. Akatov, B. S. Nikonov, B. I. Omelyanenko, S. V. Stefanovsky and J. C. Marra, Phys. Chem. Glasses, 35 (2009) 245.

[16] M. S. Aziz, F. Abdel-Wahab, A. G. Mostafa and E. M. El Agwany, J. Mater. Chem. Phys., 91 (2005) 532.

[17] A. Radu, L. Baia, W. Kiefer and S. Simon, J. Vibrational Spectroscopy, 39 (2005) 130.

[18] M. A. Marzouk, F. H. El-Batal, W. H. Eisa and N. A. Ghoneima, J. Non-Crystalline Solids, 387 (2014) 155.

[19] Ravneet Kaur, Surinder Singh and O. P. Pandey, J. Molecular Structure, 1049 (2013) 409.

[20] T. D. AbdelAziz, F. M. Ezz El-Din, H. A. El Batal and A. M. Abdelghany, J. Spectrochimica Acta Part A, (Molecular and Biomolecular Spectroscopy), 131 (2014) 501.

[21] P. Limkitjaroenporn, J. Kaewkhao, P. Limsuwan and W. Chewpraditkul, J. Physics and Chemistry of Solids, 72 (2011) 245.

[22] L. Baia, R. Stefan, J. Popp, S. Simon and W. Kiefer, J. Non-Cryst. Solids, 324 (2003) 109.

[23] R. Iordanova, V. Dimitrov, Y. Dimitriev and D. Klissurski, J. Non-Cryst. Solids, 180 (1994) 58.

[24] S. Shailajha, K. Geetha, P. Vasantharani and S. P. Sheik Abdul Kadhar, J. Spectrochimica Acta Part A, (Molecular and Biomolecular Spectroscopy), 138 (2015) 846.

[25] Yasser B. Saddeek and M. S. Gaafar, J. Materials Chemistry and Physics, 115 (2009) 280.

[26] A. M. Abdel-Ghany, A. A. Bendary, T. Z. Abou-Elnasr, M. Y. Hassaan and A. G. Mostafa, J. Nature and Science, 12 (8) (2014) 153.

[27] N. F. Mott, E. A. Davis, " Electronic processes in Non-Crystalline Materials ", Clarendon, Oxford, (1979).

[28] TG. VM. Rao, AR. Kumar and MR. Reddy, J. Non-Cryst. Solids, 356 (2012) 25.

[29] CM. Kramjce, IP. Studenyak and MV. Kurik, J. Non-Cryst. Solids, 355 (2009) 54.

[30] M. Zanini and J. Tauc, J. Non-Cryst. Solids, 23 (1977) 349.

[31] A. Agarwal, V. P. Seth, S. Sanghi, P. S. Gahlot, and D. R. Goyal, Radiation Effects & Defects in Solids, 158 (2003) 793.

[32] Ch. Rajasree and Rao. D. Krishna, J. Non-Cryst. Solids, 357 (2011) 836.

[33] S. R. Elliott, adv. Phys., 18 (1987) 41.

[34] S. R. Elliott, adv. Phys., 36 (2) (1987) 135.

[35] V. C. Veeranna Gowda and R. V. Anavenka, Solid Stat. Ionics, 176 (2005) 1393.

[36] G. Little Flower, G. Sahaya Baskaran, M. Srinivasa Reddy and N. Veeraiah, J. Physica B, 393 (2007) 72.

[37] D. E. Day, J. Non-Cryst. Solids, 21 (1976) 343.

[38] E. Mansour, J. Physica B, 362 (2005) 88.

[39] J. C. Giantini and J. V. Zancheha, J. Non-Cryst. Solids, 34 (1979) 419.